Charge generation in polymer-fullerene bulk-heterojunction solar cells

Feng Gao and Olle Inganäs

Original Publication:

Feng Gao and Olle Inganäs, Charge generation in polymer-fullerene bulk-heterojunction solar cells, 2014, Physical Chemistry, Chemical Physics - PCCP, (16), 38, 20291-20304.
http://dx.doi.org/10.1039/c4cp01814a

Charge generation in polymer-fullerene bulk-heterojunction solar cells

Feng Gao* and Olle Inganäs*

Biomolecular and Organic Electronics, IFM and Center of Organic Electronics,

Linköping University, Linköping SE-581 83, Sweden

E-mail: fenga@ifm.liu.se (F.G.) and ois@ifm.liu.se (O.I.)

Abstract

Charge generation in organic solar cells is a fundamental yet heavily debated issue. This article gives a balanced review of different mechanisms proposed to explain efficient charge generation in polymer-fullerene bulk-heterojunction solar cells. We discuss the effect of charge-transfer states, excess energy, external electric field, temperature, disorder of the materials, and delocalisation of the charge carriers on charge generation. Although a general consensus has not been reached yet, recent findings, based on both steady-state and transient measurements, have significantly advanced our understanding of this process.

1. Introduction

The power conversion efficiency of polymer solar cells, made from a blend of conjugated polymer and soluble fullerene, has increased from around 1% to over 9% in the past two decades.[1–8] These improvements have been mainly driven by significant progresses in materials synthesis and device engineering. In spite of the great success in device efficiency, many fundamental issues concerning basic operational mechanisms of these devices remain unknown or controversial, limiting further improvement of the device performance. Among others, charge generation and charge recombination might be two most fundamental yet most debated issues.[9–17]

The difficulty in understanding charge generation in PSCs is rooted in the low dielectric constant of organic materials. Low dielectric constant results in weak dielectric screening of the Coulombic attraction. As a result, a strongly bound electron-hole pair (known as an exciton) is generated upon light absorption, which is different from the case in inorganic materials, where free charge carriers are generated. The exciton has high binding energy due to Coulombic attraction, typically 0.2–0.5 eV.[18–20]

At the interfaces between the polymer and fullerene, strongly-bound excitons might dissociate, contributing to charge carrier generation. The electrons will be transferred to the electronegative acceptor, provided that the singlet exciton binding energy (E_B^{exc}) is overcome by this charge transfer process. This requirement is often satisfied by an energetic offset between the donor and acceptor lowest unoccupied molecular orbitals (LUMOs). After electron transfer, the resulting electron-hole pairs still experience Coulombic attraction because donor and acceptor phases are physically close to each other at the interfaces.

This Coulombically bound electron-hole state at the interfaces is known as charge-transfer (CT) state (Figure 1). The binding energy of the CT state (E_B^{CT}) was reported to be in

the range of 0.1–0.5 eV,[21–23] which is significantly larger than the thermal energy at room temperature (~ 25 meV). Then a fundamental question arises: what is the driving force for the CT state to split into free charge carriers, contributing to the photocurrent? This question has been puzzling the PSC community since the birth of PSCs.[24–26] There have been different mechanisms proposed to answer this question, with conflicting evidence for different opinions.

In this article, we aim to give a balanced review of these different mechanisms as well as their strength and weakness. We focus on charge generation, while charge recombination is only discussed where necessary. We understand that charge recombination is equally important as charge generation in PSCs, and recent findings suggest that kinetics (rather than thermodynamics) can prevent charge recombination and hence increase the device performance.[27,28] We start with experimental observations of CT states from both absorption and emission measurements. This is followed by spectroscopic evidence that free charge carriers are generated in the range of 100 femtoseconds in highly efficient blends. Then we focus on the long-lasting debate whether excess energy provided by the charge transfer process helps to separate CT states. We further discuss possible driving forces in the case of charge generation through relaxed CT states. In the last part of the article, we present a recently proposed mechanism, which claims that electron delocalisation in fullerene clusters plays an important role in charge generation. Throughout this article, we focus on the fullerene acceptor. This limitation reflects the very success of the fullerene acceptor in generating high efficiency in PSCs, not yet demonstrated with the alternative acceptors. The readers who are interested in other acceptors like polymers, nanocrystals, or perylene diimides are referred to some recent articles.[29–34]

2. From charge-transfer states to free charge carriers

2.1. Experimental observation of the charge-transfer state

The existence of the CT state has been demonstrated experimentally using different techniques, which probe the absorption or emission of the CT state. Both absorption and emission of the CT state show a red-shift compared with those of the individual components, because the CT state lies below the bandgap of the individual components (Figure 1).

Absorption

The absorption of the CT state requires that the electron in the donor highest occupied molecular orbital ($HOMO_D$) is directly excited into the acceptor $LUMO_A$. Since the wave function overlap between two different materials is small, the absorption coefficient of the CT state is very low. As a result, highly sensitive approaches such as photothermal deflection spectroscopy (PDS) have to be employed.[35] PDS measures the absorption by measuring the change in refractive index due to heating of the surrounding medium by light absorption in the sample. By comparing PDS signal of the polymer:fullerene blend with those of the individual components, weak absorption from the CT state was observed (Figure 2a), indicating interaction between polymer and fullerene in the ground state.[35–37]

In addition to PDS, we can also detect the CT state absorption by measuring the external quantum efficiency (EQE) of the solar cell in the CT state absorption regime, where neither polymer nor fullerene absorbs. The EQE in the CT state absorption regime results from the photocurrent generated by absorption of the CT state. A highly sensitive technique to measure the EQE in this regime is Fourier-transform photocurrent spectroscopy (FTPS).[37] In FPTS measurements, the solar-cell sample is used as an external detector of a Fourier-transform infrared spectrometer. Another approach to detect the weak photocurrent generated by directly exciting the CT state is to measure the EQE using an optical chopper, a lock-in amplifier and an infrared detector.[38] Both techniques demonstrated photocurrent signal below the bandgap of pristine materials, indicating absorption from the CT state.[37–41]

Photoluminescence

Photon absorption by the polymer (fullerene) generates excitons, which transfer electrons to the fullerene and leave holes in the polymer (or the other way around). The electrons in the fullerene might radiatively recombine with the holes in the polymer at the donor/acceptor interfaces, generating additional photoluminescence (PL) which is absent in the PL spectra of the individual components. The PL of the CT state was reported as early as 1997, when Hasharoni et al. observed weak near-infrared PL signals in the blend of MEH-PPV and fullerene (see Figure 3 for chemical structures of the molecules mentioned in this article).[42] Later on, this additional PL signal from the CT state was also observed in many other materials combinations (Figure 2b).[43–45] Although the PL of the individual components is significantly quenched by mixing with each other, the residual intensities are still comparable with that of the CT state. As a result, the measured spectrum is usually composed of the PL from both the pristine materials and CT states.[45–47]

Electroluminescence

In addition to PL, emission from the CT state was also observed in electroluminescence (EL), where injected electrons and holes recombine at the interfaces between the donor and acceptor. CT state EL was first reported by Kim et al.,[48] and then also observed by other groups (Figure 2c).[46,47,49] Although the EL of the CT state is in the same spectral range as the PL, the EL peak usually shows slight redshift compared with the PL peak.[50] In addition, the EL peak could also show slight blueshift with increasing injection current or applied voltage.[45] One explanation for this behaviour is that in EL the electrons and holes have enough time to relax to the more-ordered regions (with lower energy) to meet and recombine.

2.2. Ultrafast generation of free charge carriers

The time window in which free charge carriers are generated can be determined with the help of transient absorption (TA) measurements. TA is a time-resolved pump-probe technique, which examines the transmission difference before and after the pump excitation. After the

sample is pumped from the ground state to the excited states, the excited species might go through optical transitions to higher lying states due to photon absorption of the probe pulse. As a result, non-emissive species (e.g. polarons and triplet excitons) can be probed using this technique. The challenging aspect of this technique is the assignment of an absorption signal to a specific excited species, since the absorption of different excited species might be overlapping. Hence quantum-chemical calculations and/or global fittings of TA spectra are usually required to assist the identification of different species.

Ultrafast charge transfer (~ 45 fs) from polymer to fullerene was observed more than one decade ago by Brabec et al. using pump-probe spectroscopy.[51] However, they were not able to determine whether the product of the charge transfer was bound CT states or free charge carriers. De et al.[52] and Hwang et al.[53] were among the first to be able to determine ultrafast free charge carrier generation in polymer:fullerene blends using TA measurements in the subnanosecond time regime. Both of them observed the generation of free carriers within ~ 200 ps. Later on, using the same technique, Hwang et al. were able to further determine that free charge carriers were generated within a few picoseconds in P3HT:$PC_{60}BM$ blends.[54]

Their observation of ultrafast free charge carrier generation was subsequently confirmed by themselves as well as other groups in many other highly efficient blends.[55–62] For example, Figure 4a shows two TA spectra of annealed P3HT:$PC_{60}BM$ blends with a delay of 1 ps and 1 ns after excitation, measured by Howard et al.[61] By comparing the TA spectra with the quasi-steady-state photo-induced absorption spectra (Figure 4b), they found significant amount of free charge carriers at 1 ps in the sample. Recently, Grancini et al. observed the generation of free charge carries within 50 fs for the PCPDTBT:$PC_{60}BM$ device using sub-20 fs pump-probe spectroscopy.[63] From these recent spectroscopic measurements, e.g. the work by Grancini et al., it is usually believed that both bound CT states and free charge carriers are

immediately (~ 50 fs) generated, with the bound CT states most probably decaying to the ground states at later time scales.

In addition to TA measurements, ultrafast generation of free charge carriers was also confirmed by other techniques. Parkinson et al. employed optical-pump terahertz-probe spectroscopy to investigate the time-resolved conductivity dynamics of photoexcited P3HT:$PC_{60}BM$ blends, where the generation of free charge carriers with 100 fs was observed.[64] Studies of fullerene blends with alternating donor-acceptor copolymers of fluorene or phenylene using THz spectroscopy likewise indicated rapid charge generation.[65,66]

2.3. Dissociation of the CT state into free charge carriers

In the previous two subsections, we have discussed the existence of the CT state as well as ultrafast generation of free charge carriers. However, how the CT state dissociates into free charge carriers has been difficult to understand. Before we summarise the controversial debates on the dissociation of the CT state, we first examine the energy diagram of the processes involved in the separation, which is shown in Figure 5.

As discussed earlier, at the donor/acceptor interface, the electron will be transferred to the acceptor and the hole will be left in the donor, forming the CT state. In general, the CT state will be generated with excess thermal energy (ΔG_{CT}) due to the energy difference between the exciton and the CT state. The CT state with excess thermal energy is referred to as a hot CT state (CT_n). At this stage, two competing processes can happen. (1) The hot CT state can directly dissociate into the charge-separated (CS) states, generating free carriers. (2a) The hot CT state can thermally relax to the lowest lying CT state (CT_1), and then (2b) dissociate into the CS state, contributing to the photocurrent. A long-lasting debate is whether charge carriers are generated from the hot CT state or relaxed CT state? If generated from the relaxed CT state, what is the driving force to split the bound CT state? We will summarize different views and related experimental evidence concerning this debate.

2.3.1. Dissociation via the hot CT state

Since the CT state is generated with excess energy, it was proposed that this excess energy helps to dissociate the hot CT states directly to the free carriers before they thermalise to the ground (thermally relaxed) CT states.[67] In this hot CT state theory, the primary kinetic competition is between the thermalisation and the dissociation. As an internal conversion process, the thermalisation process is ultrafast, usually on the order of several hundred femtoseconds.[68] To be comparable with this ultrafast process, the dissociation from this hot CT state is supposed to be on the same time scale at least. Indeed, based on the TA measurements it has been suggested that free carriers could be generated in the range of 50 fs.[63] In the hot CT state theory, once relaxed to the ground CT states, the polaron pairs will primarily recombine as they do not have enough driving force to overcome the Coulombic attraction between each other under normal device operation conditions.

Ohkita et al. employed TA measurements to investigate a series of polythiophene:fullerene blends, trying to find the relation between the yield of charge carriers and the excess energy.[67] The authors found that the yield of the dissociated polarons varied by two orders depending on polythiophenes used, in spite of efficient PL quenching for all the blends. They observed a strong dependence of the yield of dissociated polarons on the energy difference between the singlet exciton and the dissociated polarons. Based on this observation, they proposed that the excess energy after the exciton dissociation provide extra kinetic energy for the CT state dissociation.[67] This hot CT state theory was further supported by their subsequent work on other polymer:fullerene blends as well as polymer:perylene diimide blends (Figure 6).[69–74]

In addition to the above work, there are some other reports supporting the hot CT state theory. For example, the sub-bandgap CT excitation was reported to generate polarons which are more localized compared with those from the above-gap excitation, implying the

importance of the excess thermal energy.[22] In the experiment, the authors compared the absorption and photocurrent under different photon energies, and found that the above-gap excitation was more effective in producing the photocurrent. This was basically an internal quantum efficiency (IQE) measurement.

Recently, Grancini *et al.* also addressed the hot CT state in PCPDTBT:$PC_{60}BM$ blends with the help of TA measurements.[63] They found that excitons split within the first 50 fs, creating both relaxed CT states and free charge carriers, depending on the excess energy. For high-energy excitation (with a large amount of excess energy), high-lying singlet states were found to convert into hot CT states, due to stronger coupling between high-energy singlets and hot CT states. This process effectively enhances the charge generation efficiency. Instead, the relaxed CT state would be a loss channel for the photocurrent. In addition, they also measured the IQE of the device, and found that IQE is wavelength-dependent, showing increasing values (by a factor of two) with increasing excitation energies. The wavelength-dependent IQE would be a direct proof for the importance of hot CT states in charge carrier generation.

However, accurate determination of IQE is not easy, since complex structure and potential imperfections of the device stack make the determination of absorption in the active layer difficult.[75] Scharber as well as Armin et al. commented on the IQE measurement by Grancini et al., and claimed that the IQE is independent of the wavelength across the absorption spectrum of the blend.[76,77] Grancini *et al.* acknowledged the difficulty in obtaining accurate IQE due to interference and parasitic absorptions. They further made a planar device, which is simplified in terms of optical effects.[78] They demonstrated that the IQE of the planar device also depends on the photon energies.

2.3.2. Dissociation via the relaxed CT state

Indeed, in spite of the difficulty in accurately determining IQE, the dependence of the IQE on wavelength might be the simplest yet most straightforward way to investigate the role of the hot CT state in charge carrier generation. Compared with the relatively small (if any) variation of IQE in the pristine materials absorption regime, determination of IQE in the CT absorption regime would help to clarify this debate, as significantly small IQE would be expected in that regime if hot CT state plays a critical role. Instead, wavelength-independent IQE values would indicate that the free charge carriers are generated from relaxed CT states.

Lee et al. investigated the IQE of two model polymer:fullerene blends, and found that the IQE stays almost constant into the low energy regime where only direct CT photoexcitation exists.[79] They further demonstrated that the dependence of photocurrent on temperature is not affected by the excitation energy either. In addition, by adjusting the incident intensity of above-gap excitation and below-gap excitation so that these two excitations give the same short-circuit current, they found overlapping current-voltage (*J*-*V*) curves. This observation is consistent with the report by Hofstad et al., who found that normalised EQE spectra (extending to the CT absorption regime) under different bias overlap with each other.[80] All these experimental data serves as evidence that the excess thermal energy plays negligible role in the CT state separation.

Very recently, Vandewal et al. further demonstrated that charge carriers are generated exclusively from the relaxed CT states, rather than hot CT states, for a range of materials combinations.[81] They employed the time-delayed-collection-field (TDCF) technique to investigate the field dependence of carrier generation.[82] TDCF is analogous to a pump-probe experiment with optical pumping and an electrical probe. During the experiment, the sample is kept at a constant pre-bias when pumped by a short laser pulse. After a certain delay time (e.g. 10 ns) following the optical pumping, the bias is switched to a collection voltage (e.g. -3V), which is supposed to be large enough to extract all remaining free charge carriers while

small enough at the same time to ensure negligible leakage current. By performing the experiment under different pre-biases, the authors found that the extracted free charges are independent of excitation energy. This indicates that free charge carrier generation at different biases does not depend on the excess energy provided by incident light.

Although above experiments seem to provide evidence against hot CT state theory, one may still argue that the below-gap excitation energy used in these experiments does not necessarily produce lowest-energy relaxed CT states exclusively. Even with below-gap excitation, most CT states might still be relatively hot, since vibrationally excited CT states will be produced due to the reorganization of the atoms following photon absorption. Unless relaxed CT states are accessed exclusively, it is difficult to demonstrate that relaxed CT states are exclusive precursors for charge carrier generation. However, direct measurement of absorption from the lowest-energy CT state is very challenging due to low probability of thermal population of vibrationally excited ground state. Vandewal et al. found an alternative approach to do this. They reconstructed the absorption spectrum in this low-energy regime by measuring radiative decay from the thermally-relaxed CT manifold.[81] The measurement of the absorption and the EQE in the low-energy regime enabled the authors to determine the IQE of relaxed CT excitation. They found a constant IQE irrespective of the excitation energy for different materials combinations they investigated (Figure 7). Based on this, they concluded that free charge carrier generation is exclusively from the relaxed CT state, rather than from the hot CT state.

In addition, Howard et al. compared the TA measurements between regiorandom (RRa) P3HT:$PC_{60}BM$ and regioregular (RR) P3HT:$PC_{60}BM$ blends.[61] They found that the free carrier generation is much lower in the RRa P3HT:$PC_{60}BM$ blend, which has larger ΔG_{CT}. This is another piece of evidence against the hot CT mechanism, which predicts that the system with larger excess energy would generate more free charge carriers. Instead, the

authors proposed that the ultrafast free carrier generation is dependent on the morphology, with more ordered samples showing higher free carrier generation yield.

2.4. Driving force in the case of dissociation via the relaxed CT state

If the hot CT state is the exclusive precursor for free charge carrier generation, ultrafast free charge carrier generation is self-explaining. However, if the relaxed CT state is the exclusive precursor for free charge carrier generation, what is the driving force for CT state separation? Based on Coulomb's law, the binding energy of the CT state is

$$E_b = \frac{q^2}{4\pi\varepsilon_r\varepsilon_0 a} \quad (1)$$

where q is the elementary charge, ε_r is the relative permittivity, ε_0 is the vacuum permittivity, and a is the distance between the electron and hole. ε_r is assumed to be the macroscopic value of the active layer, which is around 3-4, and a is assumed to be in the range of 1-2 nm. As a result, E_B estimated from these assumptions is around 0.2-0.5 eV. Actually the assumptions of ε_r and a are close to those for excitons in pure materials. And hence it is not surprising that the estimated binding energy is in the same range as the excitons in individual components, where an energetic offset between the donor and acceptor LUMOs is required to assist the exciton dissociation. Therefore, such a high binding energy for the CT state requires a driving force to split them into free charge carriers.

2.4.1. Braun-Onsager model

A commonly used quantitative model for considering the CT state separation is the Braun-Onsager (BO) theory.[83–85] The BO theory gives a quantitative description of the dependence of the CT state dissociation rate (k_{diss}) on a set of measurable parameters, including the electric field (F), the mobility of electrons (μ_e) and holes (μ_h), the temperature (T), etc.

$$k_{diss}(a,T,F) = \frac{q}{\varepsilon_r \varepsilon_0}\langle \mu_e + \mu_h \rangle \frac{3}{4\pi a^3} e^{-E_b/k_B T} J_1(2\sqrt{-2b})/(\sqrt{-2b}) \qquad (2)$$

where $\langle ... \rangle$ denotes the spatial average, $k_B T$ is the thermal energy, $b = q^3 F/(8\pi\varepsilon_r\varepsilon_0 k_B^2 T^2)$, and J_1 is the Bessel function of order one $J_1(2\sqrt{-2b})/(\sqrt{-2b}) = 1 + b + b^2/3 + b^3/18 + \cdots$. Although there are also some other modifications to the BO theory describing the escape yield of charge pairs,[86–88] they generally depend on the same set of parameters.

The BO theory has been employed to quantitatively simulate *J-V* characteristics of the BHJ PSCs based on the drift-diffusion equations.[89–92] In macroscopic modeling, the electron and hole mobilities are usually fitted from the space-charge-limited current regime of the single-carrier devices, while the geminate recombination (GR) rate is used as a fitting parameter. The experimental current-voltage curves could be reproduced for some less efficient polymer:fullerene blends, e.g. MDMO-PPV:$PC_{60}BM$ blends.[9]

However, in order to get a good fitting to the measured *J-V* characteristics, a low GR rate on the order of 10^4 – 10^6 s^{-1} was often used.[89,90] This is in contrast with the TA measurement, where a GR rate larger than 10^7 s^{-1} was usually reported.[62] In addition, we are not aware of a report on reproducing *J-V* curves of highly efficient PSCs, indicating that there might be some intrinsic limitations using the BO theory to quantitatively explain the CT state separation. For example, disorder, which is intrinsic to semiconducting polymers, is not included in the BO theory. Albrecht and Bässler pointed out that disorder could significantly modify the dissociation rate of charge pairs.[93] As a result, it has been shown that the BO theory performs poorly when compared to more realistic Monte Carlo (MC) simulations.[93,94] Another parameter which is neglected in the BO theory is the morphology, which plays a critical role in determining charge generation in PSCs.[95,96] In addition, the BO theory focuses on how the CT state is separated, and ignores how it is created. Considering ultrafast generation of free

charge carriers (on the timescale < 100 fs), the dynamics of the CT state creation and free charge carrier generation might be difficult to separate.

2.4.2. The effect of the electric field

Although the BO theory does not seem to be a quantitative theory to explain the free charge carrier generation in PSCs, there are many attempts trying to investigate whether the parameters suggested by the BO theory qualitatively explain the experimental observations. Among these parameters, the effect of the electric field on the dissociation of the CT state is relatively easy to investigate.

Recall that the CT state shows PL, though the quantum efficiency is low. Therefore, one approach to probe the effect of the electric field on the CT state separation is to examine how the field quenches the CT state PL. Indeed, it has been demonstrated from the PL measurement that the CT state emission could be quenched upon the application of the electric field.[23,45,47,50] However, it was also found that usually a large field (over 10^8 V/m, corresponding to 10 V over a 100 nm thick device) is needed to effectively quench the CT state emission, while under the usual device operation condition (~ 10^7 V/m), the quenching is marginal. This observation contradicts the fact that the polymer:fullerene blends usually give high photocurrent at the short-circuit condition, which indicates efficient CT state separation under the normal electric field. One argument could be that the emissive CT states do not represent all the CT states. Instead, the non-emissive CT states, which might have different field dependence, contribute to the photocurrent.[50]

Another technique to investigate the effect of the electric field is field-dependent TA measurements. Shuttle et al. reported that in the P3HT:$PC_{60}BM$ system, no obvious variation in initial (~ 0.5 μs) polaron signal amplitude was observed under different biases. This indicated that the field had little effect on the carrier photogeneration.[97] A similar experiment was performed by the same group on PCPDTBT:$PC_{70}BM$ devices. Consistent with their

previous results, no field-dependent charge photogeneration was observed.[98] These experiments implied that the electric field (in the device operation regime) does not help the dissociation of the CT state.

Marsh *et al.* performed similar experiments on a working P3HT:$PC_{60}BM$ device, with wider time range and in a sufficiently low intensity regime relevant to the operation condition of PSCs under solar illumination.[99] Their result showed that the electric field (in the device operation regime) increased the life time of the charge carriers, indicating that the electric field-assisted dissociation of the CT state helped to enhance charge photogeneration. Similar measurements were performed on PCDTBT:$PC_{70}BM$ devices by the same group, with results similar to the findings on P3HT:$PC_{60}BM$ devices.[100] As we can see, similar experiments on the same materials by two different groups gave conflicting results. The discrepancy might arise from the fact that the field dependence occurs at early times that are beyond the resolution of the TA measurements by Shuttle et al. Another possibility is that these two groups measured different P3HT:$PC_{60}BM$ samples. The charge generation mechanisms of P3HT:$PC_{60}BM$ depend heavily on a range of factors, including the annealing temperature, the degradation of the sample, the regioregularity of P3HT, etc.[62]

A further method to investigate the field dependence is the TDCF technique, as we have introduced previously. A critical issue in this experiment is the determination of the delay time between the pre-bias and the extraction voltage. The delay time is supposed to be longer than the CT state lifetime yet shorter than charge extraction time. The TDCF technique revealed that different materials combinations have different field dependence of charge carrier generation (Figure 8). For example, MEH-PPV:$PC_{60}BM$ blends and PCPDTBT:$PC_{70}BM$ blends show significant field dependence while P3HT:$PC_{60}BM$ blends and PBDTTPD:$PC_{60}BM$ blends show negligible field dependence.[81,101–103]

An indirect approach to examine the field dependence of the CT state separation is to measure charge carrier densities and their lifetimes, which can be determined by charge extraction and transient photovoltage decay measurements, respectively.[104] During charge extraction measurements, the device under illumination is initially biased at an applied voltage. Then the device is shorted and at the same time the illumination is switched off. With the assumption that all the free charge carriers can be extracted out of the device at short-circuit conditions, the carrier density at this applied voltage can be estimated by measuring the discharging current. During photovoltage decay measurements, the device is held at open-circuit conditions under continuous background illumination, on which a weak pulsed optical perturbation is then applied. The charge carrier lifetime is estimated by fitting the decay (presumably monoexponential) of the transient photovoltage induced by the perturbation. With carrier densities and their lifetimes as well as an assumption of recombination mechanism (e.g. bimolecular recombination), the recombination current can be estimated at different biases. The difference between the saturation current and recombination current is supposed to overlap with the measured *J*-*V* curve if no field-dependent charge generation is involved. Indeed, for P3HT:$PC_{60}BM$ devices, it was reported that there is no need to introduce any field-dependent CT state separation.[105] We emphasize that this approach is an indirect method, as it probes the bimolecular recombination of separated charge carriers, rather than directly probes the CT state dynamics.

2.4.3. The effect of the temperature

Although temperature might be an important parameter to help us understand the CT state separation process, the temperature dependence is more complicated than the field dependence as at least hopping rates of charge carriers also depend on temperature. Based on the BO theory, the CT state dissociation rate will exponentially decrease with decreasing temperature, implying orders of magnitude decrease in the photocurrent at lower temperatures.

However, significant amount of photocurrent was observed at low temperatures.[106,107] One explanation could be that the lifetime of the CT state increases with decreasing temperature, so that the dissociation probability is still high at low temperatures.[108] Unfortunately, recent measurement of the CT state PL decay at different temperatures indicated that CT state lifetime is independent of temperature over a wide temperature range (from room temperature to 5 K).[109]

Other than examining temperature dependence of the photocurrent, it might be also informative to examine temperature dependence of the open-circuit voltage (V_{OC}), where all charge carriers recombine and no charge transport issue is involved. If charge carrier generation is temperature-independent, V_{OC} increases with decreasing temperature due to larger carrier densities at lower temperatures. This behaviour has been reported for different blends at temperatures above 150 K.[110,111] However, if charge carrier generation probability decreases with decreasing temperature, this will cancel out increased carrier densities mentioned above, and make the V_{OC} flatten and even decrease at some point. This behaviour has been observed in un-annealed P3HT:$PC_{60}BM$ devices but not analysed in details.[112] A careful analysis of temperature-dependent V_{OC} in a wide temperature range might provide a unique approach to understand the effect of temperature on charge carrier generation.

2.4.4. The effect of the mobility

We have mentioned that the electron/hole mobilities of the devices are usually fitted from the space-charge-limited current regime of the single-carrier devices. However, some reports pointed out that the mobilities obtained in this way might significantly underestimate the real local mobilities during the CT separation process. Veldman et al. noticed that $PC_{60}BM$ aggregates often form in the devices with a high $PC_{60}BM$ concentration.[47] They used a high mobility value (~ 0.1 $cm^2\ V^{-1}\ s^{-1}$) measured in microcrystalline $PC_{60}BM$ powder to represent the local electron mobility, and achieved good fits of their data. More recently,

Burke and McGehee argued that it is the high local mobility (e.g. measured by time resolved terahertz spectroscopy) that is critical to the CT state separation process.[113] They employed high mobilities (on the order of 1-10 cm^2 V^{-1} s^{-1}) in kinetic MC simulations, and found that these high mobilities could well reproduce efficient charge carrier generation.

2.4.5. The effect of the disorder

In the BO theory, energetic and spatial disorder is neglected. However, both theoretical and experimental results indicate that disorder is important in helping the charge generation. As mentioned before, with the help of MC simulation, in 1995 Albrecht and Bässler pointed out that charge generation could be aided by the disorder.[93] More recently, quantum chemistry calculations have indicated that disorder at the interfaces between the donor and acceptor may be structured in a way that favors charge separation.[114,115] This disorder at the interface has been shown by kinetic MC simulation to be quite effective at separating CT states, contributing to high internal quantum efficiency.[113,116] In addition, the electron and hole forming the CT state have typically not relaxed within the disorder-broadened density of states (DOS). With the help of kinetic MC simulation, Eersel et al. demonstrated that the remaining binding energy could be overcome by further relaxation in the DOS.[117] Although this process could involve a substantial loss of the energy due to the relaxation process, they claimed that the energy loss could be minimized with careful materials design.

Further demonstration of the effect of the disorder on the CT state separation was reported recently by Vithanage et al.[118] They employed the Time Resolved Electric Field-Induced Second Harmonic (TREFISH) technique to probe the electric field dynamics with subpicosecond time resolution. Second-harmonic generation is a non-linear optical process where two photons are summed into a photon of double the energy. The yield of this process depends on the electric field, and hence serves as a proxy of changes in electric field. They then used a parallel-plate capacitor model where the electron/hole could drift due to the

applied bias to reconstruct the electron-hole distance and their mobilities. They found that charge pairs separate rapidly through diffusion (~3 nm at 10 ps and > 5 nm at 100 ps), although these charge pairs are closely bound (< 1 nm) when they are generated. The results were further rationalised by MC simulations, where an energetic disorder-induced DOS was assumed.

In a recent work, this approach has been extended to combine TREFISH measurements with time-of-flight measurements in a full account of the cooling of charge carriers due to hopping within the disordered DOS. MC simulation has successfully been used to map these processes in a unified model.[119] The material in this case was a TQ1:$PC_{70}BM$ blend, and results and models are consistent with the transient absorption results reported in ref. 120 as well as the transient microwave conductivity results.[121]

2.5. The role of charge delocalisation on free charge generation

Up to now, we have discussed the possibility of dissociation through hot CT states, which explain well the ultrafast charge carrier generation observed in TA measurements and field-independent generation observed in a range of techniques. However, the fact that the dissociation probability is independent of photon energy seems to contradict this hot CT mechanism, which would predict an excitation energy-dependent carrier generation. We have also discussed the possibility of dissociation through relaxed CT states. In spite of intensive research in this direction, there is no consensus concerning the driving force to split the CT state in this case. Instead, some recent reports reinvestigated the basic assumption (a distance of 1-2 nm between the electron on the acceptor and the hole on the donor) in calculating the binding energy of the CT state, and found that the charge delocalisation might play a critical role on free charge carrier generation.

Bakulin et al. employed a pump-push photocurrent (PPP) technique to investigate a range of materials combinations, and demonstrated the importance of hole delocalisation

along the polymer chain.[122] In the PPP technique, a working device is first pumped by visible light, creating separated charges and/or localised CT states. The pump excitation is followed by an infrared push pulse, which is supposed to re-excite the localised CT states into separated charges. By comparing the photocurrent before and after the push pulse, the effect of this push pulse is demonstrated. The authors observed a sharp rise in photocurrent with the arrival of the push pulse immediately after the pump pulse (within 200 fs), indicating that the push pulse interacts with a species created directly after excitation. Aided by atomistic 'many-body' modelling, they rationalized their results by hole delocalisation along the polymer chain (Figure 9a). And they acknowledged that they could not exclude the possibility of electron delocalisation along fullerene clusters, which might further help the charge separation. The importance of hole delocalisation was also highlighted by kinetic MC simulations. For example, Deibel et al. proposed that the hole delocalisation on the extended conjugation length (between 4 and 10 monomer units) is responsible for the efficient charge carrier generation.[123]

In spite of many attempts,[47,124,125] the electron delocalisation has not been unambiguously demonstrated until very recently. Gélinas et al. resolved the electron-hole distance by tracking the modulation of the optical absorption due to the electric field generated when the electron and hole separate from each other.[126] What they measured is basically an electro-absorption (EA) signal, i.e. Stark effect. They could measure the EA in the femtosecond regime, and calculate the energy stored in the electric field. Hence they could quantify the temporal electron-hole distance during the initial charge generation process. They found that an electrostatic energy as high as 200 meV is stored in the electric field within 40 fs of excitation for an efficient device, corresponding to an electron-hole distance of at least 4 nm. They also examined a poor performance device with the same donor and acceptor (fullerene) materials but with decreasing fullerene concentration. They found that although

this device was also efficient in hole generation, no EA signal was observed, indicating long range electron-hole separation is hindered due to decreased fullerene concentration (Figure 10). Based on these results, the authors proposed that electron delocalisation due to the existence of fullerene clusters is of critical importance for efficient free carrier generation (Figure 9b).[127] This finding is consistent with the ubiquitous use of fullerene in highly efficient devices, and supported by the electronic structure calculations on large fullerene clusters.[128] In addition, Falke et al. showed that coherent electron-nuclear motion might play a key role in charge delocalization over the polymer-fullerene interfaces.[129]

We note that above charge delocalisation mechanism is different from the exciton delocalisation mechanism proposed by Kaake et al., who performed TA measurements on a range of materials combinations and observed similar fast charge carrier generation (within 100 fs).[130,131] Based on the fact that this time scale is much faster than exciton diffusion time (expected to be in ps to ns regime), the authors argued that the exciton is delocalised, which is responsible for efficient charge carrier generation. Although this argument provides a possible mechanism for ultrafast carrier generation, it needs more experimental evidence to support it. In addition, this mechanism does not explain why polymer acceptor generally works worse than fullerene acceptor if exciton delocalisation is the key factor.

3. Conclusions

We reviewed the state-of-the-art knowledge on a controversial yet critical issue in polymer solar cells, i.e. charge generation. We focused on the charge separation processes at the polymer:fullerene interfaces. Although we have not had a clear answer to this controversial issue yet, recent findings, based on both steady-state and transient measurements, have significantly advanced our understanding of this process.

Even in such a controversial area, there are several findings that the community generally agree on. For example, interfacial CT states do exist in polymer:fullerene blends, as

evidenced from both absorption and luminescence measurements. In addition, a large amount of charge generation is ultrafast (in the range of 100 fs) in highly efficient blends, which has been demonstrated by TA measurements in different research groups. Field dependence of charge carrier generation seems to depend on materials combinations.

A long-lasting debate is whether charge carriers are generated through relaxed CT states or through delocalised (hot) CT states. In the former mechanism, the relaxed CT state is the exclusive precursor for free charge carriers, while in the latter, the charge generation is assisted by the excess energy inherited from the charge transfer process. Although hot CT state mechanism explains the ultrafast charge carrier generation very well, general observation of photon energy-independent IQE contradicts this mechanism. In the case of generation through relaxed CT states, there must be a driving force to split the bound states. Although parameters like electric field, temperature, mobility and disorder has been considered, there is no general consensus yet. We note that the entropic aspect of this process specifies one part of the free energy change, and contributes to understanding of charge formation also in localized systems.[132] Kinetic MC simulations indicate that also in fully disordered systems, the charge separation is entropically preferred, and can account for photocurrent generation.

Recent spectroscopic findings indicated that electrons might be delocalised in fullerene clusters, so that the electron-hole distance is much larger (~5 nm) than what we previously thought. This explains why fullerene is always used in highly efficient devices. In this mechanism, the energy loss is not intrinsic to charge generation processes, and hence could be minimised in principle. This has important implications for future materials design, and also opens up new questions. For example, it has been demonstrated in many combinations that an intermixing phase with both polymer and fullerene is crucial for efficient charge generation.[133–138] This delocalisation mechanism does not seem to give a direct answer to this

observation, and further investigation might be needed to get a complete understanding of charge generation in PSCs.

Acknowledgements

We thank Dr. Artem Bakulin for helpful discussions, Dr. Simon Gélinas and Dr. Wolfgang Tress for critical reading of the manuscript. Research on organic photovotaics at Linköping University is supported by the Science Council (VR), the Swedish Energy Agency and the Knut and Alice Wallenberg foundation (KAW). F.G. acknowledges the financial support of the European Commission under a Marie Curie Intra-European Fellowship for Career Development.

References

1. G. Yu, J. Gao, J. C. Hummelen, F. Wudl, and A. J. Heeger, *Science*, 1995, **270**, 1789 –1791.
2. G. Li, V. Shrotriya, J. Huang, Y. Yao, T. Moriarty, K. Emery, and Y. Yang, *Nat. Mater.*, 2005, **4**, 864–868.
3. J. Peet, J. Y. Kim, N. E. Coates, W. L. Ma, D. Moses, A. J. Heeger, and G. C. Bazan, *Nat. Mater.*, 2007, **6**, 497–500.
4. H.-Y. Chen, J. Hou, S. Zhang, Y. Liang, G. Yang, Y. Yang, L. Yu, Y. Wu, and G. Li, *Nat. Photonics*, 2009, **3**, 649–653.
5. Y. He, H.-Y. Chen, J. Hou, and Y. Li, *J. Am. Chem. Soc.*, 2010, **132**, 1377–1382.
6. E. Wang, L. Hou, Z. Wang, S. Hellström, F. Zhang, O. Inganäs, and M. R. Andersson, *Adv. Mater.*, 2010, **22**, 5240–5244.
7. Y. Liang, Z. Xu, J. Xia, S.-T. Tsai, Y. Wu, G. Li, C. Ray, and L. Yu, *Adv. Mater.*, 2010, **22**, E135–E138.
8. Z. He, C. Zhong, S. Su, M. Xu, H. Wu, and Y. Cao, *Nat. Photonics*, 2012, **6**, 591–595.
9. P. W. M. Blom, V. D. Mihailetchi, L. J. A. Koster, and D. E. Markov, *Adv. Mater.*, 2007, **19**, 1551–1566.
10. T. M. Clarke and J. R. Durrant, *Chem. Rev.*, 2010, **110**, 6736–6767.
11. J.-L. Brédas, J. E. Norton, J. Cornil, and V. Coropceanu, *Acc. Chem. Res.*, 2009, **42**, 1691–1699.
12. C. Deibel, T. Strobel, and V. Dyakonov, *Adv. Mater.*, 2010, **22**, 4097–4111.
13. C. Deibel and V. Dyakonov, *Rep. Prog. Phys.*, 2010, **73**, 096401.
14. C. Piliego and M. A. Loi, *J. Mater. Chem.*, 2012, **22**, 4141–4150.
15. C. Groves, *Energy Environ. Sci.*, 2013, **6**, 3202–3217.
16. R. A. J. Janssen and J. Nelson, *Adv. Mater.*, 2013, **25**, 1847–1858.
17. G. Lakhwani, A. Rao, and R. H. Friend, *Annu. Rev. Phys. Chem.*, 2014, **65**, null.
18. V. I. Arkhipov and H. Bässler, *Phys. Status Solidi – Appl. Mater. Sci.*, 2004, **201**, 1152–1187.
19. S. F. Alvarado, P. F. Seidler, D. G. Lidzey, and D. D. C. Bradley, *Phys. Rev. Lett.*, 1998, **81**, 1082–1085.
20. J. Brédas, J. Cornil, and A. J. Heeger, *Adv. Mater.*, 1996, **8**, 447–452.
21. X.-Y. Zhu, Q. Yang, and M. Muntwiler, *Acc. Chem. Res.*, 2009, **42**, 1779–1787.
22. T. Drori, C.-X. Sheng, A. Ndobe, S. Singh, J. Holt, and Z. V. Vardeny, *Phys. Rev. Lett.*, 2008, **101**, 037401.
23. M. Hallermann, S. Haneder, and E. Da Como, *Appl. Phys. Lett.*, 2008, **93**, 053307.
24. B. Kraabel, C. H. Lee, D. McBranch, D. Moses, N. S. Sariciftci, and A. J. Heeger, *Chem. Phys. Lett.*, 1993, **213**, 389–394.
25. B. Kraabel, J. C. Hummelen, D. Vacar, D. Moses, N. S. Sariciftci, A. J. Heeger, and F. Wudl, *J. Chem. Phys.*, 1996, **104**, 4267–4273.
26. B. Kraabel, D. McBranch, N. S. Sariciftci, D. Moses, and A. J. Heeger, *Phys. Rev. B*, 1994, **50**, 18543–18552.
27. C. W. Schlenker, K.-S. Chen, H.-L. Yip, C.-Z. Li, L. R. Bradshaw, S. T. Ochsenbein, F. Ding, X. S. Li, D. R. Gamelin, A. K.-Y. Jen, and D. S. Ginger, *J. Am. Chem. Soc.*, 2012, **134**, 19661–19668.
28. A. Rao, P. C. Y. Chow, S. Gélinas, C. W. Schlenker, C.-Z. Li, H.-L. Yip, A. K.-Y. Jen, D. S. Ginger, and R. H. Friend, *Nature*, 2013, **500**, 435–439.
29. C. R. McNeill and N. C. Greenham, *Adv. Mater.*, 2009, **21**, 3840–3850.
30. F. Gao, S. Ren, and J. Wang, *Energy Environ. Sci.*, 2013, **6**, 2020–2040.
31. R. Shivanna, S. Shoaee, S. Dimitrov, S. K. Kandappa, S. Rajaram, J. R. Durrant, and K. S. Narayan, *Energy Environ. Sci.*, 2013, **7**, 435–441.
32. S. Rajaram, R. Shivanna, S. K. Kandappa, and K. S. Narayan, *J. Phys. Chem. Lett.*, 2012, **3**, 2405–2408.
33. A. Sharenko, C. M. Proctor, T. S. van der Poll, Z. B. Henson, T.-Q. Nguyen, and G. C. Bazan, *Adv. Mater.*, 2013, **25**, 4403–4406.
34. X. Zhang, Z. Lu, L. Ye, C. Zhan, J. Hou, S. Zhang, B. Jiang, Y. Zhao, J. Huang, S. Zhang, Y. Liu, Q. Shi, Y. Liu, and J. Yao, *Adv. Mater.*, 2013, **25**, 5791–5797.
35. L. Goris, K. Haenen, M. Nesládek, P. Wagner, D. Vanderzande, L. Schepper, J. D'haen, L. Lutsen, and J. V. Manca, *J. Mater. Sci.*, 2005, **40**, 1413–1418.
36. J. J. Benson-Smith, L. Goris, K. Vandewal, K. Haenen, J. V. Manca, D. Vanderzande, D. D. C. Bradley, and J. Nelson, *Adv. Funct. Mater.*, 2007, **17**, 451–457.

37. L. Goris, A. Poruba, L. Hod'ákova, M. Vaněček, K. Haenen, M. Nesládek, P. Wagner, D. Vanderzande, L. De Schepper, and J. V. Manca, *Appl. Phys. Lett.*, 2006, **88**, 052113.
38. S. Ko, E. T. Hoke, L. Pandey, S. Hong, R. Mondal, C. Risko, Y. Yi, R. Noriega, M. D. McGehee, J.-L. Brédas, A. Salleo, and Z. Bao, *J. Am. Chem. Soc.*, 2012, **134**, 5222–5232.
39. K. Vandewal, K. Tvingstedt, A. Gadisa, O. Inganäs, and J. V. Manca, *Nat. Mater.*, 2009, **8**, 904–909.
40. K. Vandewal, A. Gadisa, W. D. Oosterbaan, S. Bertho, F. Banishoeib, I. Van Severen, L. Lutsen, T. J. Cleij, D. Vanderzande, and J. V. Manca, *Adv. Funct. Mater.*, 2008, **18**, 2064–2070.
41. E. T. Hoke, K. Vandewal, J. A. Bartelt, W. R. Mateker, J. D. Douglas, R. Noriega, K. R. Graham, J. M. J. Fréchet, A. Salleo, and M. D. McGehee, *Adv. Energy Mater.*, 2013, **3**, 220–230.
42. K. Hasharoni, M. Keshavarz-K, A. Sastre, R. González, C. Bellavia-Lund, Y. Greenwald, T. Swager, F. Wudl, and A. J. Heeger, *J. Chem. Phys.*, 1997, **107**, 2308–2312.
43. M. A. Loi, S. Toffanin, M. Muccini, M. Forster, U. Scherf, and M. Scharber, *Adv. Funct. Mater.*, 2007, **17**, 2111–2116.
44. M. C. Scharber, C. Lungenschmied, H.-J. Egelhaaf, G. Matt, M. Bednorz, T. Fromherz, J. Gao, D. Jarzab, and M. A. Loi, *Energy Environ. Sci.*, 2011, **4**, 5077–5083.
45. Y. Zhou, K. Tvingstedt, F. Zhang, C. Du, W. Ni, M. R. Andersson, and O. Inganäs, *Adv. Funct. Mater.*, 2009, **19**, 3293–3299.
46. K. Tvingstedt, K. Vandewal, A. Gadisa, F. Zhang, J. Manca, and O. Inganäs, *J. Am. Chem. Soc.*, 2009, **131**, 11819–11824.
47. D. Veldman, O. İpek, S. C. J. Meskers, J. Sweelssen, M. M. Koetse, S. C. Veenstra, J. M. Kroon, S. S. van Bavel, J. Loos, and R. A. J. Janssen, *J. Am. Chem. Soc.*, 2008, **130**, 7721–7735.
48. H. Kim, J. Y. Kim, S. H. Park, K. Lee, Y. Jin, J. Kim, and H. Suh, *Appl. Phys. Lett.*, 2005, **86**, 183502.
49. M. A. Faist, T. Kirchartz, W. Gong, R. S. Ashraf, I. McCulloch, J. C. de Mello, N. J. Ekins-Daukes, D. D. C. Bradley, and J. Nelson, *J. Am. Chem. Soc.*, 2012, **134**, 685–692.
50. K. Tvingstedt, K. Vandewal, F. Zhang, and O. Inganäs, *J Phys Chem C*, 2010, **114**, 21824–21832.
51. C. J. Brabec, G. Zerza, G. Cerullo, S. De Silvestri, S. Luzzati, J. C. Hummelen, and S. Sariciftci, *Chem. Phys. Lett.*, 2001, **340**, 232–236.
52. S. De, T. Pascher, M. Maiti, K. G. Jespersen, T. Kesti, F. Zhang, O. Inganäs, A. Yartsev, and V. Sundström, *J. Am. Chem. Soc.*, 2007, **129**, 8466–8472.
53. I. -W Hwang, C. Soci, D. Moses, Z. Zhu, D. Waller, R. Gaudiana, C. J. Brabec, and A. J. Heeger, *Adv. Mater.*, 2007, **19**, 2307–2312.
54. I.-W. Hwang, D. Moses, and A. J. Heeger, *J. Phys. Chem. C*, 2008, **112**, 4350–4354.
55. M. Tong, N. E. Coates, D. Moses, A. J. Heeger, S. Beaupré, and M. Leclerc, *Phys. Rev. B*, 2010, **81**, 125210.
56. J. Guo, H. Ohkita, H. Benten, and S. Ito, *J. Am. Chem. Soc.*, 2010, **132**, 6154–6164.
57. J. Guo, H. Ohkita, H. Benten, and S. Ito, *J. Am. Chem. Soc.*, 2009, **131**, 16869–16880.
58. R. A. Marsh, J. M. Hodgkiss, S. Albert-Seifried, and R. H. Friend, *Nano Lett.*, 2010, **10**, 923–930.
59. S. De, T. Kesti, M. Maiti, F. Zhang, O. Inganäs, A. Yartsev, T. Pascher, and V. Sundström, *Chem. Phys.*, 2008, **350**, 14–22.
60. S. K. Pal, T. Kesti, M. Maiti, F. Zhang, O. Inganäs, S. Hellström, M. R. Andersson, F. Oswald, F. Langa, T. Österman, T. Pascher, A. Yartsev, and V. Sundström, *J. Am. Chem. Soc.*, 2010, **132**, 12440–12451.
61. I. A. Howard, R. Mauer, M. Meister, and F. Laquai, *J. Am. Chem. Soc.*, 2010, **132**, 14866–14876.
62. I. A. Howard and F. Laquai, *Macromol. Chem. Phys.*, 2010, **211**, 2063–2070.
63. G. Grancini, M. Maiuri, D. Fazzi, A. Petrozza, H.-J. Egelhaaf, D. Brida, G. Cerullo, and G. Lanzani, *Nat. Mater.*, 2013, **12**, 29–33.
64. P. Parkinson, J. Lloyd-Hughes, M. B. Johnston, and L. M. Herz, *Phys. Rev. B*, 2008, **78**, 115321.
65. H. Němec, H.-K. Nienhuys, F. Zhang, O. Inganäs, A. Yartsev, and V. Sundström, *J. Phys. Chem. C*, 2008, **112**, 6558–6563.
66. H. Němec, H.-K. Nienhuys, E. Perzon, F. Zhang, O. Inganäs, P. Kužel, and V. Sundström, *Phys. Rev. B*, 2009, **79**, 245326.
67. H. Ohkita, S. Cook, Y. Astuti, W. Duffy, S. Tierney, W. Zhang, M. Heeney, I. McCulloch, J. Nelson, D. D. C. Bradley, and J. R. Durrant, *J. Am. Chem. Soc.*, 2008, **130**, 3030–3042.

68. T. Virgili, D. Marinotto, C. Manzoni, G. Cerullo, and G. Lanzani, *Phys. Rev. Lett.*, 2005, **94**, 117402.
69. T. M. Clarke, A. M. Ballantyne, J. Nelson, D. D. C. Bradley, and J. R. Durrant, *Adv. Funct. Mater.*, 2008, **18**, 4029–4035.
70. T. M. Clarke, A. M. Ballantyne, S. Tierney, M. Heeney, W. Duffy, I. McCulloch, J. Nelson, and J. R. Durrant, *J. Phys. Chem. C*, 2010, **114**, 8068–8075.
71. S. Shoaee, Z. An, X. Zhang, S. Barlow, S. R. Marder, W. Duffy, M. Heeney, I. McCulloch, and J. R. Durrant, *Chem. Commun.*, 2009, **45**, 5445–5447.
72. S. D. Dimitrov and J. R. Durrant, *Chem. Mater.*, 2014, **26**, 616–630.
73. S. D. Dimitrov, A. A. Bakulin, C. B. Nielsen, B. C. Schroeder, J. Du, H. Bronstein, I. McCulloch, R. H. Friend, and J. R. Durrant, *J. Am. Chem. Soc.*, 2012, **134**, 18189–18192.
74. A. A. Bakulin, S. D. Dimitrov, A. Rao, P. C. Y. Chow, C. B. Nielsen, B. C. Schroeder, I. McCulloch, H. J. Bakker, J. R. Durrant, and R. H. Friend, *J. Phys. Chem. Lett.*, 2012, **4**, 209–215.
75. L. A. A. Pettersson, L. S. Roman, and O. Inganäs, *J. Appl. Phys.*, 1999, **86**, 487.
76. M. Scharber, *Nat. Mater.*, 2013, **12**, 594–594.
77. A. Armin, Y. Zhang, P. L. Burn, P. Meredith, and A. Pivrikas, *Nat. Mater.*, 2013, **12**, 593–593.
78. G. Grancini, M. Binda, L. Criante, S. Perissinotto, M. Maiuri, D. Fazzi, A. Petrozza, H.-J. Egelhaaf, D. Brida, G. Cerullo, and G. Lanzani, *Nat. Mater.*, 2013, **12**, 594–595.
79. J. Lee, K. Vandewal, S. R. Yost, M. E. Bahlke, L. Goris, M. A. Baldo, J. V. Manca, and T. V. Voorhis, *J. Am. Chem. Soc.*, 2010, **132**, 11878–11880.
80. T. G. J. van der Hofstad, D. Di Nuzzo, M. van den Berg, R. A. J. Janssen, and S. C. J. Meskers, *Adv. Energy Mater.*, 2012, **2**, 1095–1099.
81. K. Vandewal, S. Albrecht, E. T. Hoke, K. R. Graham, J. Widmer, J. D. Douglas, M. Schubert, W. R. Mateker, J. T. Bloking, G. F. Burkhard, A. Sellinger, J. M. J. Fréchet, A. Amassian, M. K. Riede, M. D. McGehee, D. Neher, and A. Salleo, *Nat. Mater.*, 2014, **13**, 63–68.
82. T. Offermans, S. C. J. Meskers, and R. A. J. Janssen, *J. Appl. Phys.*, 2006, **100**, 074509.
83. L. Onsager, *Phys. Rev.*, 1938, **54**, 554–557.
84. C. L. Braun, *J. Chem. Phys.*, 1984, **80**, 4157.
85. L. Onsager, *J. Chem. Phys.*, 1934, **2**, 599.
86. K. M. Hong and J. Noolandi, *J. Chem. Phys.*, 1978, **69**, 5026.
87. M. Wojcik and M. Tachiya, *Radiat. Phys. Chem.*, 2005, **74**, 132–138.
88. M. Wojcik and M. Tachiya, *J. Chem. Phys.*, 2009, **130**, 104107.
89. L. J. A. Koster, V. D. Mihailetchi, and P. W. M. Blom, *Appl. Phys. Lett.*, 2006, **88**, 052104.
90. L. J. A. Koster, E. C. P. Smits, V. D. Mihailetchi, and P. W. M. Blom, *Phys. Rev. B*, 2005, **72**, 085205.
91. C. Deibel, A. Wagenpfahl, and V. Dyakonov, *Phys. Status Solidi - Rapid Res. Lett.*, 2008, **2**, 175–177.
92. V. D. Mihailetchi, H. X. Xie, B. de Boer, L. J. A. Koster, and P. W. M. Blom, *Adv. Funct. Mater.*, 2006, **16**, 699–708.
93. U. Albrecht and H. Bässler, *Chem. Phys. Lett.*, 1995, **235**, 389–393.
94. C. Groves, J. C. Blakesley, and N. C. Greenham, *Nano Lett.*, 2010, **10**, 1063–1069.
95. P. K. Watkins, A. B. Walker, and G. L. B. Verschoor, *Nano Lett.*, 2005, **5**, 1814–1818.
96. R. A. Marsh, C. Groves, and N. C. Greenham, *J. Appl. Phys.*, 2007, **101**, 083509.
97. C. G. Shuttle, B. O'Regan, A. M. Ballantyne, J. Nelson, D. D. C. Bradley, and J. R. Durrant, *Phys. Rev. B*, 2008, **78**, 113201.
98. F. C. Jamieson, T. Agostinelli, H. Azimi, J. Nelson, and J. R. Durrant, *J. Phys. Chem. Lett.*, 2010, **1**, 3306–3310.
99. R. A. Marsh, J. M. Hodgkiss, and R. H. Friend, *Adv. Mater.*, 2010, **22**, 3672–3676.
100. R. H. Friend, M. Phillips, A. Rao, M. W. B. Wilson, Z. Li, and C. R. McNeill, *Faraday Discuss*, 2012, **155**, 339–348.
101. S. Albrecht, W. Schindler, J. Kurpiers, J. Kniepert, J. C. Blakesley, I. Dumsch, S. Allard, K. Fostiropoulos, U. Scherf, and D. Neher, *J. Phys. Chem. Lett.*, 2012, **3**, 640–645.
102. J. Kniepert, M. Schubert, J. C. Blakesley, and D. Neher, *J. Phys. Chem. Lett.*, 2011, **2**, 700–705.
103. M. Mingebach, S. Walter, V. Dyakonov, and C. Deibel, *Appl. Phys. Lett.*, 2012, **100**, 193302.

104. A. Maurano, C. G. Shuttle, R. Hamilton, A. M. Ballantyne, J. Nelson, W. Zhang, M. Heeney, and J. R. Durrant, *J. Phys. Chem. C*, 2011, **115**, 5947–5957.
105. C. G. Shuttle, R. Hamilton, B. C. O'Regan, J. Nelson, and J. R. Durrant, *Proc. Natl. Acad. Sci.*, 2010, **107**, 16448–16452.
106. D. Chirvase, Z. Chiguvare, M. Knipper, J. Parisi, V. Dyakonov, and J. C. Hummelen, *J. Appl. Phys.*, 2003, **93**, 3376–3383.
107. H. H. P. Gommans, M. Kemerink, J. M. Kramer, and R. a. J. Janssen, *Appl. Phys. Lett.*, 2005, **87**, 122104.
108. F. Gao, J. Wang, J. C. Blakesley, I. Hwang, Z. Li, and N. C. Greenham, *Adv. Energy Mater.*, 2012, **2**, 956–961.
109. D. Jarzab, F. Cordella, J. Gao, M. Scharber, H.-J. Egelhaaf, and M. A. Loi, *Adv. Energy Mater.*, 2011, **1**, 604–609.
110. K. Vandewal, K. Tvingstedt, A. Gadisa, O. Inganäs, and J. V. Manca, *Phys. Rev. B*, 2010, **81**, 125204.
111. S. R. Cowan, A. Roy, and A. J. Heeger, *Phys. Rev. B*, 2010, **82**, 245207.
112. A. K. Thakur, G. Wantz, G. Garcia-Belmonte, J. Bisquert, and L. Hirsch, *Sol. Energy Mater. Sol. Cells*, 2011, **95**, 2131–2135.
113. T. M. Burke and M. D. McGehee, *Adv. Mater.*, 2014, **26**, 1923–1928.
114. D. P. McMahon, D. L. Cheung, and A. Troisi, *J. Phys. Chem. Lett.*, 2011, **2**, 2737–2741.
115. G. D'Avino, S. Mothy, L. Muccioli, C. Zannoni, L. Wang, J. Cornil, D. Beljonne, and F. Castet, *J. Phys. Chem. C*, 2013, **117**, 12981–12990.
116. C. Groves, *Energy Environ. Sci.*, 2013, **6**, 1546–1551.
117. H. van Eersel, R. A. J. Janssen, and M. Kemerink, *Adv. Funct. Mater.*, 2012, **22**, 2700–2708.
118. D. A. Vithanage, A. Devižis, V. Abramavičius, Y. Infahsaeng, D. Abramavičius, R. C. I. MacKenzie, P. E. Keivanidis, A. Yartsev, D. Hertel, J. Nelson, V. Sundström, and V. Gulbinas, *Nat. Commun.*, 2013, **4**.
119. A. Melianas, V. Pranculis, A. Devižis, V. Gulbinas, O. Inganäs, and M. Kemerink, *Adv. Funct. Mater.*, Accepted.
120. L. M. Andersson, A. Melianas, Y. Infahasaeng, Z. Tang, A. Yartsev, O. Inganäs, and V. Sundström, *J. Phys. Chem. Lett.*, 2013, **4**, 2069–2072.
121. D. H. K. Murthy, A. Melianas, Z. Tang, G. Juška, K. Arlauskas, F. Zhang, L. D. A. Siebbeles, O. Inganäs, and T. J. Savenije, *Adv. Funct. Mater.*, 2013, **23**, 4262–4268.
122. A. A. Bakulin, A. Rao, V. G. Pavelyev, P. H. M. van Loosdrecht, M. S. Pshenichnikov, D. Niedzialek, J. Cornil, D. Beljonne, and R. H. Friend, *Science*, 2012, **335**, 1340–1344.
123. C. Deibel, T. Strobel, and V. Dyakonov, *Phys. Rev. Lett.*, 2009, **103**, 036402.
124. K. G. Jespersen, F. Zhang, A. Gadisa, V. Sundström, A. Yartsev, and O. Inganäs, *Org. Electron.*, 2006, **7**, 235–242.
125. D. H. K. Murthy, M. Gao, M. J. W. Vermeulen, L. D. A. Siebbeles, and T. J. Savenije, *J Phys Chem C*, 2012, **116**, 9214–9220.
126. S. Gélinas, A. Rao, A. Kumar, S. L. Smith, A. W. Chin, J. Clark, T. S. van der Poll, G. C. Bazan, and R. H. Friend, *Science*, 2014, **343**, 512–516.
127. F. C. Jamieson, E. B. Domingo, T. McCarthy-Ward, M. Heeney, N. Stingelin, and J. R. Durrant, *Chem. Sci.*, 2012, **3**, 485–492.
128. B. M. Savoie, A. Rao, A. A. Bakulin, S. Gelinas, B. Movaghar, R. H. Friend, T. J. Marks, and M. A. Ratner, *J. Am. Chem. Soc.*, 2014, **136**, 2876–2884.
129. S. M. Falke, C. A. Rozzi, D. Brida, M. Maiuri, M. Amato, E. Sommer, A. D. Sio, A. Rubio, G. Cerullo, E. Molinari, and C. Lienau, *Science*, 2014, **344**, 1001–1005.
130. L. G. Kaake, D. Moses, and A. J. Heeger, *J. Phys. Chem. Lett.*, 2013, **4**, 2264–2268.
131. L. G. Kaake, J. J. Jasieniak, R. C. Bakus, G. C. Welch, D. Moses, G. C. Bazan, and A. J. Heeger, *J. Am. Chem. Soc.*, 2012, **134**, 19828–19838.
132. B. A. Gregg, *J. Phys. Chem. Lett.*, 2011, **2**, 3013–3015.
133. N. C. Cates, R. Gysel, Z. Beiley, C. E. Miller, M. F. Toney, M. Heeney, I. McCulloch, and M. D. McGehee, *Nano Lett.*, 2009, **9**, 4153–4157.
134. A. C. Mayer, M. F. Toney, S. R. Scully, J. Rivnay, C. J. Brabec, M. Scharber, M. Koppe, M. Heeney, I. McCulloch, and M. D. McGehee, *Adv. Funct. Mater.*, 2009, **19**, 1173–1179.

135. J. A. Bartelt, Z. M. Beiley, E. T. Hoke, W. R. Mateker, J. D. Douglas, B. A. Collins, J. R. Tumbleston, K. R. Graham, A. Amassian, H. Ade, J. M. J. Fréchet, M. F. Toney, and M. D. McGehee, *Adv. Energy Mater.*, 2013, **3**, 364–374.
136. N. C. Cates, R. Gysel, J. E. P. Dahl, A. Sellinger, and M. D. McGehee, *Chem. Mater.*, 2010, **22**, 3543–3548.
137. N. D. Treat, M. A. Brady, G. Smith, M. F. Toney, E. J. Kramer, C. J. Hawker, and M. L. Chabinyc, *Adv. Energy Mater.*, 2011, **1**, 82–89.
138. P. Westacott, J. R. Tumbleston, S. Shoaee, S. Fearn, J. H. Bannock, J. B. Gilchrist, S. Heutz, J. deMello, M. Heeney, H. Ade, J. Durrant, D. S. McPhail, and N. Stingelin, *Energy Environ. Sci.*, 2013, **6**, 2756–2764.

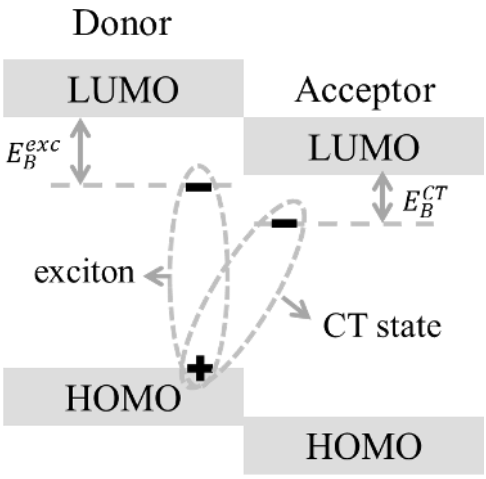

Figure 1 Schematic illustration of the CT state formation, with the exciton and CT state binding energies included. For simplicity, the binding energies are shown relative to the LUMOs.

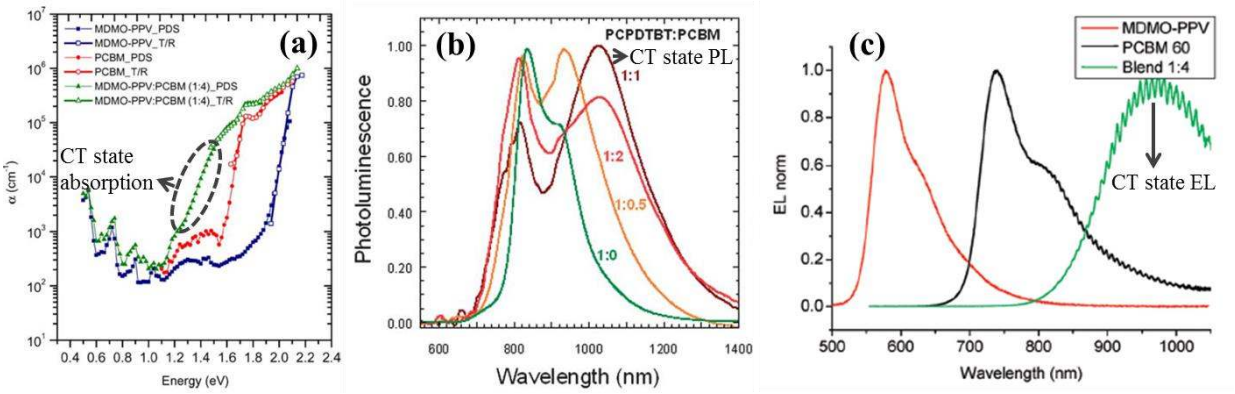

Figure 2 Observation of the CT state from absorption and emission measurements. (a) PDS measurements revealed additional absorption signal (due to CT state absorption) compared with those of the pure components. (b) In addition to the residual PL from the pure components, a red-shifted PL peak due to CT state emission appeared in the polymer:fullerene blend. (c) In the EL spectrum of the blend, only CT state emission was observed, while that from the pure components disappeared. (a) Reproduced with permission from Ref. 35, Copyright 2005, Springer. (b) Reproduced with permission from Ref. 44, Copyright 2011, The Royal Society of Chemistry. (c) Reproduced with permission from Ref. 46, Copyright 2009, American Chemical Society.

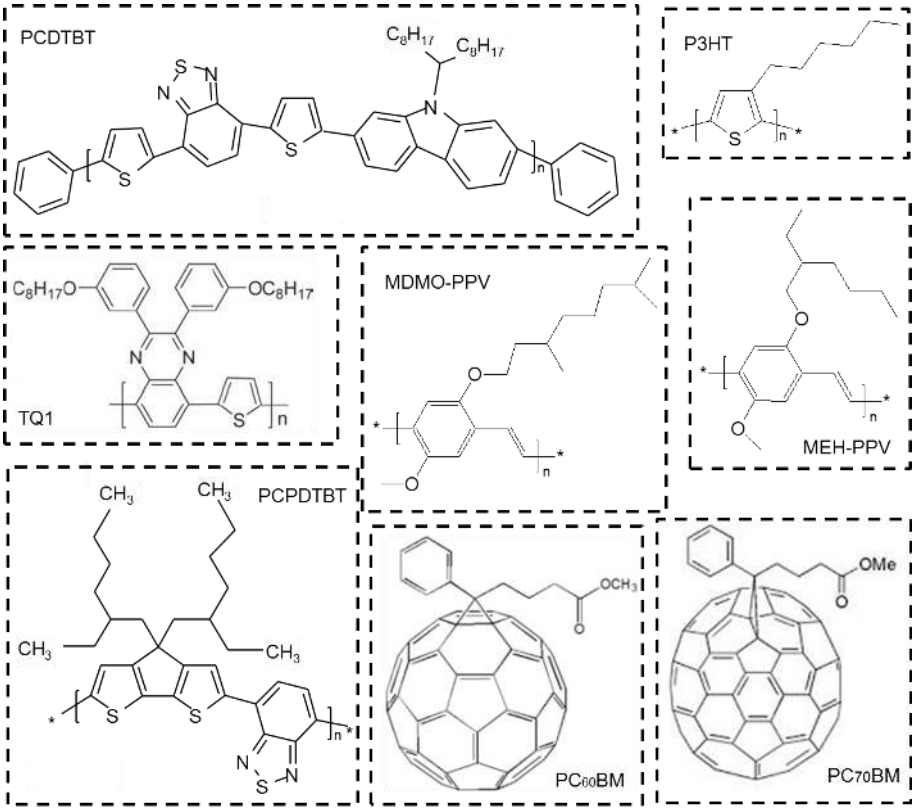

Figure 3 Chemical structures of some of the polymers and fullerene derivatives mentioned in this article.

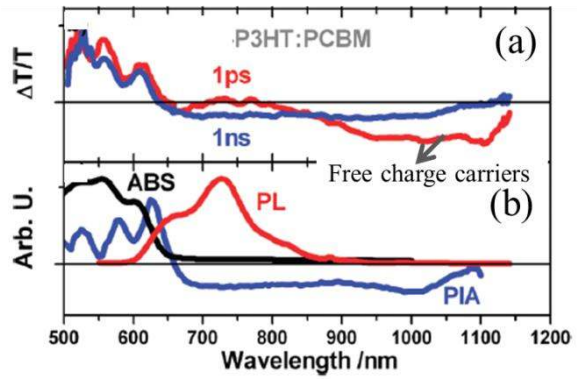

Figure 4 Ultrafast free charge carrier generation in annealed P3HT:$PC_{60}BM$ blends. (a) TA spectra measured at 1 ps (red line) and 1 ns (blue line) after excitation. (b) Absorption and PL of the pure P3HT film as well as quasi-steady-state photo-induced absorption (PIA) spectrum of the blend (measured at 80 K). The PIA signal is from free charge carriers. By comparing the PIA signal in panel b with the TA signal in panel a, it is clear that significant amount of free charge carriers are already present in the blend film 1ps after the excitation. Reproduced with permission from Ref. 61, Copyright 2010, American Chemical Society.

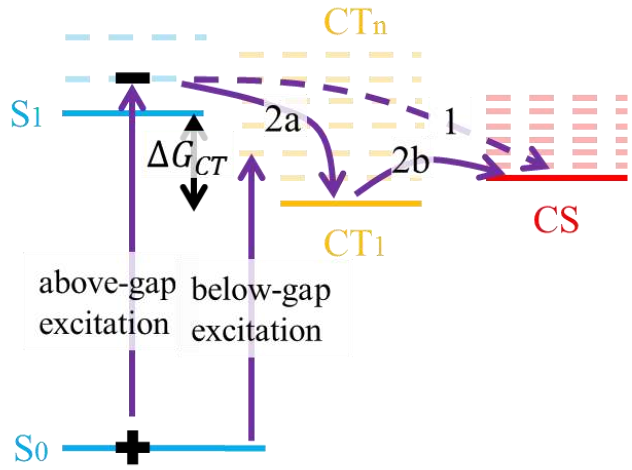

Figure 5 Energy diagram summarizing the debate concerning charge generation. Photon absorption generates singlet excitons (S_1), which dissociate at the interfaces, forming CT states with excess thermal energy (ΔG_{CT}), known as hot CT States. The hot CT state can (1) directly dissociate into the charge-separated (CS) state, or (2a) first thermalize to the relaxed CT state (CT_1) and then (2b) dissociate into the CS state. Above-gap and below-gap excitation is also shown in the figure.

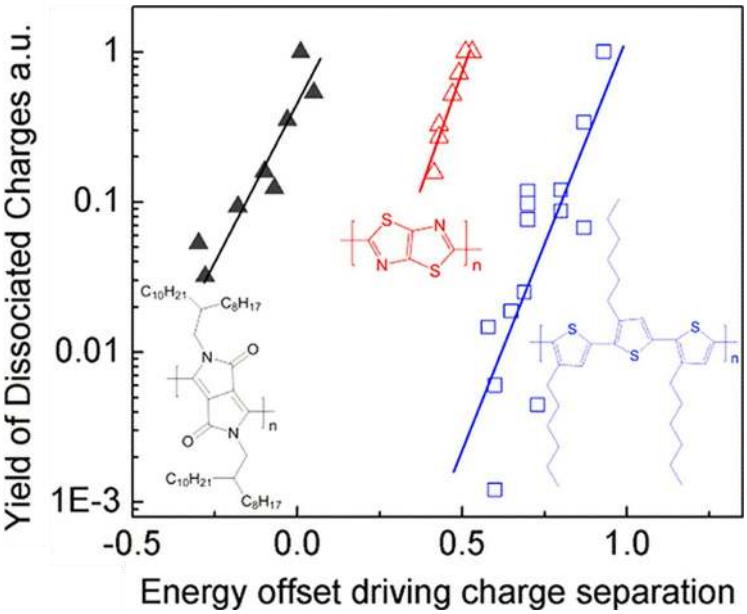

Figure 6 For three different series of polymer:fullerene blends, the yield of dissociated charges increases with increasing energy offset, implying the importance of hot CT state. Reproduced with permission from Ref. 72, Copyright 2013, American Chemical Society.

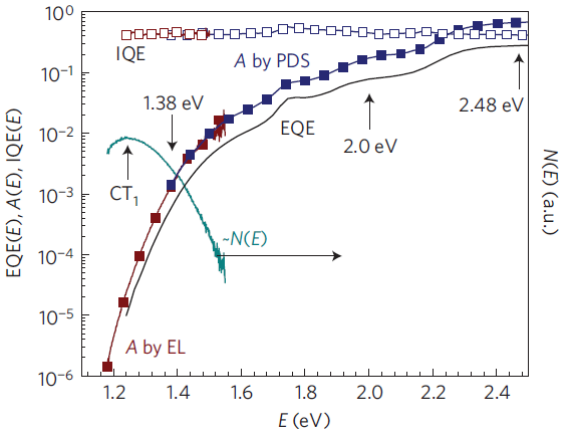

Figure 7 Constant IQE across a wide range of excitation energy for MEH-PPV:$PC_{60}BM$ blends. This implies that excess energy plays a negligible effect on the charge generation process and that free carriers are generated from relaxed CT states. Reproduced with permission from Ref. 81, Copyright 2013, Nature Publishing Group.

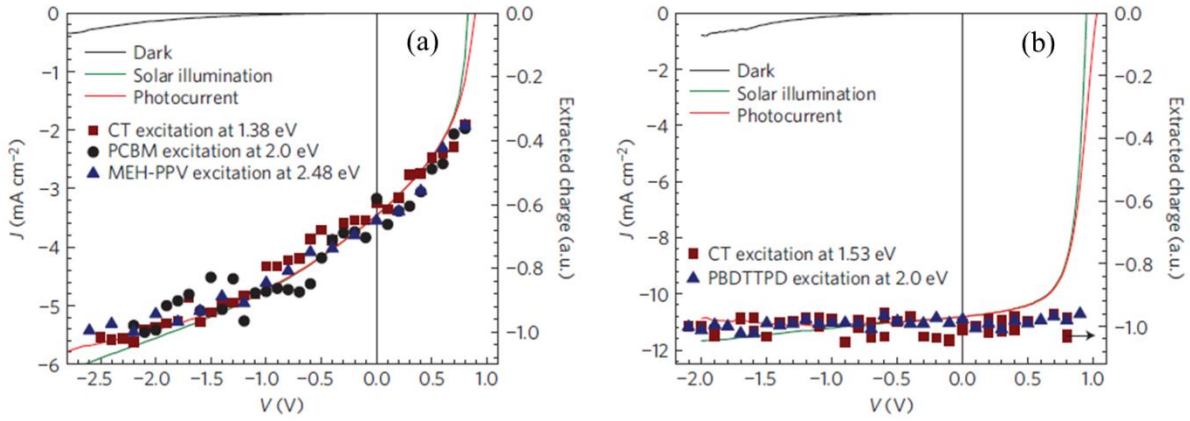

Figure 8 Different blends show different field dependence of charge carrier generation, as revealed by TDCF measurements. The charge carrier generation in (a) MEH-PPV:$PC_{60}BM$ blends is field dependent, while that in (b) PCPDTBT:PC70BM blends is field independent. Reproduced with permission from Ref. 81, Copyright 2013, Nature Publishing Group.

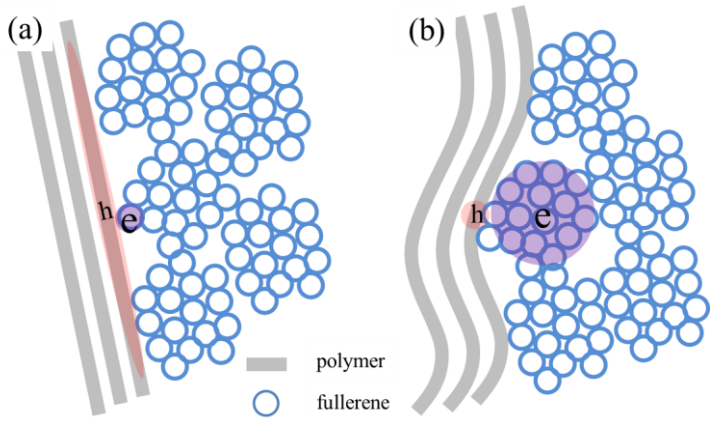

Figure 9 Schematic illustration of (a) hole delocalisation along the polymer chain and (b) electron delocalisation in the fullerene cluster.

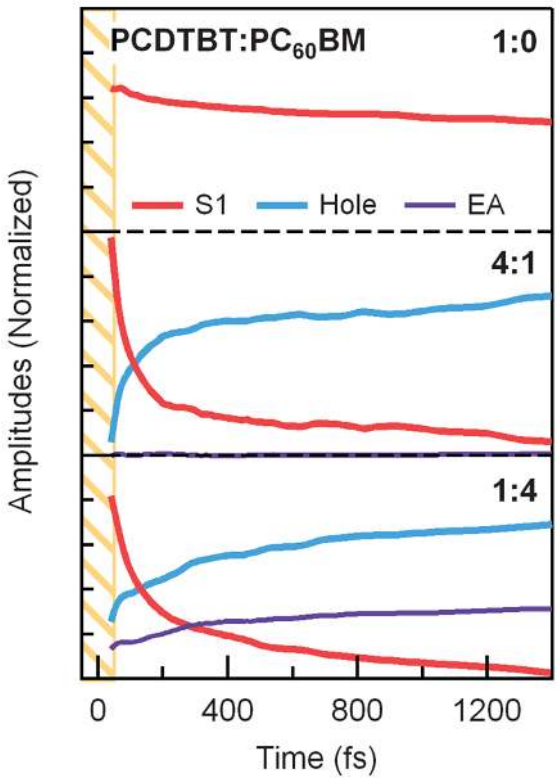

Figure 10 For the fullerene rich device (1:4), EA signal was observed at 40 fs, indicating long-range separation of electron-hole pair within a short time. For the polymer rich device, although hole signal was observed, no EA signal was detected, indicating the generation of bound electron-hole pairs. This result highlights the critical role of fullerene clusters in charge generation. Reproduced with permission from Ref. 126, Copyright 2014, The American Association for the Advancement of Science.